Investigation of Size Effects to the Mixing Performance on the X-shaped Micro-Channels

Shu-Min Tu[1], Shuichi Torii[1] and Yang-Cheng Shih[2]
[1] Department of Mechanical System Engineering,
Kumamoto University, Japan
[2] Department of Energy, Refrigeration and Air-Condition Engineering
National Taipei University of Technology, Taiwan

ABSTRACT

Due to the developing of micro-electro-mechanical-system, MEMS, the fabrication of the microminiaturization devices becomes obviously important. The advances in the basic understanding of fluid physics have opened an era of application of fluid dynamics systems using micro-channels. The purpose of this study is to research the flow transport phenomenon by employing different kinds of micro-channel sizing in X-shaped micro-channels. As the working fluid, water is injected to micro-channel at different mass flow rate. Over a wide range of flow condition, $1.06 < Re < 514$, in X-shaped micro-channels, the mixture performances of numerical simulation, flow visualization, and temperature distribution remain the same. At the same mass flow rate as the Reynolds number below 112.53, the biggest channel size had the slowest flow velocity and got the best mixing performance; as the Reynolds number above 112.53, the smaller the channel sizing, the lower the pressure drops and the faster velocity becomes. The transition form early from laminar flow, the unsteady flow is an advantage for mixing in the limited mixing area, therefore 0.7 mm got the best mixing performance. It is clear that the size of the channel plays an important role in the X-shaped micro-channels.

Keywords: X-shaped micro-channels; flow visualization; mixing performance

1. INTRODUCTION

Nowadays micro-electro-mechanical systems and micro-total analysis systems are having an important impact in many engineering applications, such as medicine and bioengineering, computer technology and thermal transfer engineering. The use of convective heat transfer in cooling micro-channel has been proposed over the last decades. Understanding the internal flow effects on the fluid flow temperature gradient, velocity vector and pressure drop helps to improve the design of those devices. For designing the mixer, the traditional normal sized channels can be stirred or used in other ways to form the turbulence flow for mixing. However, with very low Reynolds number and flow velocity in micro-channels, mixing takes relatively long and hard time. Devising a highly efficient and stable micro mixer is a critical issue of the micro fluid researching. The main concern of the study of converging, mixing and diverging processes in micro-channels concentrates on enhancing mixing performance such as stretched and folded fluids to generate chaotic advection and increased the interfacial area or incorporated obstructions within the micro-channel to break up and recombine the

flow. The key factors that affect the mixing performance include channel size and shape, flow field pattern, flow path length, fluid pressure, etc.

A number of investigations of the micro-channel mixer internal flow have been widely carried out before. Zhang and Lin [1], discussed the concentration and orientation of fiber in a turbulent T-shaped branching channel flow. They announced that, at low Reynolds number, fiber concentration was high in the flow separation regions and fiber orientation throughout the channel was widely distributed with a slight preference of aligning along the horizontal axis. Y-shaped channel has been studied by Chang and Yang [2] and Guo [3]. Chang and Yang employed the lattice Boltzmann method to simulate the thermal mixing efficiency of 2-D, incompressible, steady-state low Reynolds number flows in a Y-shaped channel. The effects of introducing a staggered arrangement of wave-like and circular obstacles into the mixing section of the Y-shaped channel were systematically examined. Guo investigated the effects of bed discordance on the flow patterns at Y-shaped open channel confluences by using a 3-D numerical simulation. It proved that the model can undertake quantitative assessment of the flow at confluences. The results indicated that there were a lot of differences between the Y-shaped confluence and asymmetrical confluence. The discordant bed height plays an important role at the Y-shaped junction.

Shakhawat Hossain and M.A. Ansari. [4] evaluated the mixing and flow structures in micro-channels with different geometries: zig-zag; square-wave; and curved. The results showed that the square-wave micro-channel yields the best mixing performance; the curved and the zig-zag micro-channel show nearly the same performance for most Reynolds number. Robin H. Liu and Mark A.Stremler [5] also studied the serpentine micro-channels; they designed with a C-shaped repeating unit as a means of implementing chaotic advection to passively enhance fluid mixing. They disclosed that mixing rates in the serpentine channel at the higher Reynolds numbers were consistent with the occurrence of chaotic advection.

Sasawat and Muammer [6] investigated the "size effects" on the material flow curve of thin sheet metals under hydraulic bulge testing conditions. The ratio of the sheet thickness to the material grain size ($N = t_0/d$) was used as a parameter to characterize the interactive effects between the specimen and the grain sizes at the micro-scales, while the ratio of the bulge die diameter to the sheet thickness ($M = Dc/t_0$) was used to represent the effect of the feature size in the bulge test. The results of the bulge tests at different scales showed a decrease in the material flow curve with decreasing N value from 5.5 to 3.0, and with decreasing M value from 1961 to 191. However, as M value was decreased further from 191 to 49, an inversed relation between the flow curve and M value was observed; that is, the flow curve was found to increase with decreasing M value from 191 to 49. Wang and Peng [7] experimentally studied the forced convection of liquids (water and methanol) in micro-channels of rectangular cross-section. They observed that the heat transfer behavior in laminar and transition regions was quite unusual and complicated, and was strongly influenced by liquid temperature, velocity and micro channel size.

Many previous investigations have been concentrated upon the mixing performance on the T-type and Y-type micro mixer or upon the size effect on the micro-channel, but no references discuss with the channel sizing effect to the mixing performance on the micro mixer. This article analyzes the fluid flow transport phenomenon in X-shaped micro-channels numerical simulation, flow visualization, and temperature distribution. Fluid flow transport phenomenon in X-shaped micro-channels consists of converging, mixing and diverging flows. A 2-D modeling approach is adopted to examine the complex flow on the X-typed micro mixer. Our goal is to design a mixer by studying the effects of channel sizing. Since mixing in passive mixer occurs primarily by diffusion, reducing the mixing area is generally beneficial for faster mixing.

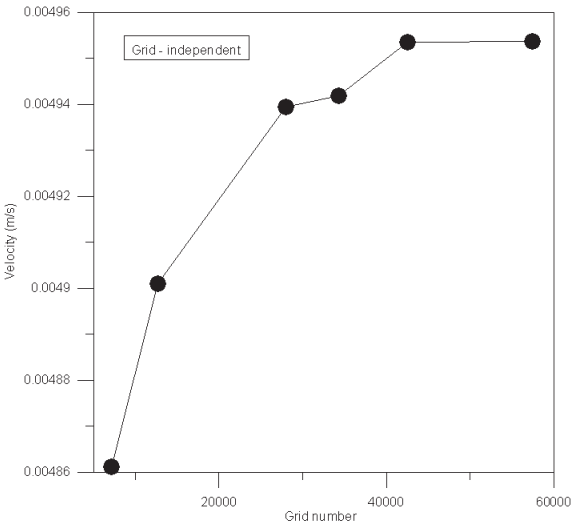

Figure 1: Grid-independent until

2. EXPERIMENTAL METHODS

2.1. NUMERICAL SIMULATION

The micro mixer designs were modeled and simulated by using the CFD FLUENT software (ANSYS, Inc.). To minimize effects of meshing on mixing, the mesh density was increased by grid-independent until (as show in Fig. 1). Six different structured grid systems, wherein the number of grids ranges from 7190 to 57408, were tested for each micro-channel. Finally, from the results of the grid-independent test, 42536 were selected (relative error in velocity equal to 0.006%) as the optimal number of grids.

The dimension of the X-shaped micro-channels for *x*-direction was 20 mm with *Lc*, 40 mm with *Lm* and 20 mm with *Ld*; for *y*-direction, the scale length was determined by the different channel sizing, the channel sizing with 0.7, 0.8, 0.9, 1, 1.1, 1.2, and 1.3 mm was employed in this study. The converging and diverging angles are designed by 90°. The following assumptions were imposed in the formulation of the problem solving based on the characteristics of the flow: incompressible, continuum, no-slip boundary condition, a fully developed convection with constant fluid properties (H_2O water) in the upstream region. The governing equations include continuity, momentum, and energy equations, which obey the principle of conservation that can be expressed in the following general form,

$$\frac{\partial}{\partial t}(\rho\phi) + \nabla \bullet \left(\rho\vec{V}\phi - \Gamma_{\phi,eff}\nabla\phi\right) = S_\phi \tag{1}$$

ρ is the density, ϕ is the dependent variable, $\vec{V}$ is the velocity vector, $\Gamma_{\phi,eff}$ is the effective diffusion coefficient, and S_ϕ is the source term. The diffusion-convection term of Eq. (1) is discretized by the second-order upwind scheme and the implicit method is used to discretize the transient term. After Eq. (1) is discretized, the general discretized equation can be written as (2),

$$a_p\phi_p = \sum a_{nb}\phi_{nb} + b \tag{2}$$

where a_p and a_{nb} are discretized coefficients, and b is the discretized source term. In Eq. (2), subscript p represents the grid point under consideration and nb indicates the neighbors of grid point p. By employing the iterative scheme of a point implicit (Gauss-Seidel) linear equation solver in conjunction with an algebraic multigrid (AMG) method, the pressure and velocity, fields can be solved from Eq. (2).

During the iterative procedure, the SIMPLEC (Semi-Implicit Method for Pressure - Linked Equations - Consistent) algorithm was employed to solve the pressure-velocity coupling equations. The boundary condition of both outlets pressure was set to be 0 Pa. The solutions are considered to have attained the convergence when the value of the relative residual is at most 10^{-6}.

2.2. APPARATUS SETUP

The present study selects X-shaped channels having the same width and height of converging, mixing and diverging passages in the order of 0.7, 1, and 1.3 mm, a 2-D flow in X-shaped channels with free stream. Fig. 2 illustrates a schematic diagram of the experimental apparatus. The micro mixer is made by acrylic for observing the flow pattern visualization. The test section is distinguished to converging area: Lc = 20 mm, mixing area: Lm = 40 mm and diverging area: Ld = 20mm. The converging and diverging angles are designed by 90°.

2.3. FLOW VISUALIZATION

During the testing, one syringe was filled with dyeing water, blue, while the other was red. Using syringe pumps (AS ONE syringe pump systems, SPE-1, speed range from 0.006 to 6 mm/min), the two syringes were driven at flow rates ranging form 0.00141 Kg/s (Re = 1.106) to 0.70522 Kg/s (Re = 508.006). The Reynolds number in (3) is valid for the common channel, whereas the X-shaped micro-channels has two inlet and both the inlet channels are characterized by half the Reynolds number.

$$\mathrm{Re} = \frac{\rho v d}{\mu} \tag{3}$$

Two series of experiments were conducted: One supplied the same mass flow rate in both Inlet 1 and Inlet 2 but increasing it in each case (Case 1, Case 2, Case 4 and Case 7), and the other supplied the different mass flow rate to Inlet 1 and Inlet 2 (Case 3, Case5 and Case6)

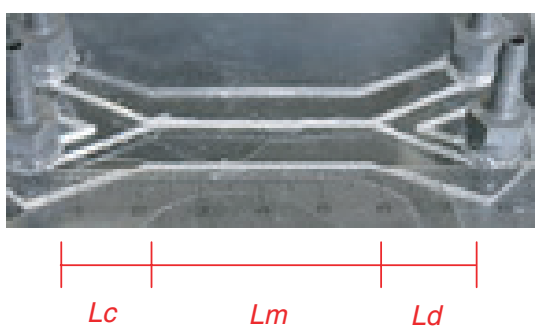

Figure 2: X-shaped micro-channels

Table 1: Mass flow rate in each case (Kg/s)

	Inlet 1	Inlet 2	Total
Case 1	0.0007	0.0007	0.0014
Case 2	0.0070	0.0070	0.0141
Case 3	0.0070	0.0705	0.0775
Case 4	0.0705	0.0705	0.1410
Case 5	0.0070	0.3526	0.3596
Case 6	0.0705	0.3526	0.4231
Case 7	0.3526	0.3526	0.7052

for understanding the mixing preference (As Table 1). The Mixing of the two fluids was observed by using Digital single-lens reflex camera (Canon EOS Kiss3) plus the macro lens (Canon EF 100 mm *f*/2.8 L Macro IS USM).

2.4. TEMPERATURE MEASUREMENT

For the temperature measurement, the initial conditions of two inputs are controlled at 290K and 300 K respectively. The temperatures are maintained by the water circulator baths (EYELA uni thermo ace NCC-1100). In order to reduce the heat loss to the surroundings (around 300 K), all syringes, pipes, and mixer are covered with 1 inch thermal protector. Type-K thermocouples, accuracy ± 0.75%, are applied to measure the temperatures in both outputs. The thermocouples are connected to a data acquisition system (TAKARA THERMISTOR TE E830), and then recorded the temperature at the time when the mixing processing is at 5 minutes.

3. RESULTS AND DISSUSSION

The simulation results and images from different channel size in Case 2 are shown in Fig. 3 and Fig. 4 with different values of Reynolds number. In the design of the mixer, the flow visualization is usually used to obtain the mixing segment, providing a picture of how mixing progresses as the fluids move downstream. In case 2, with the same supplied mass flow rate in Inlet 1 and Inlet 2 as 0.007 Kg/s, the smaller channel size has the lower the pressure drop and faster flow velocity. Fig. 5 represents the relationship between pressure drop to Reynolds number and Fig. 6 represents the velocity to mass flow rate of Inlet 1 in case1, 2, 4 and 7. As Shakhawat Hossain [4] declared that at a very low Reynolds number, micro mixers can be classified into two categories: active and passive. Active micro mixers use additional structures or external sources to stir the fluids. Passive micro mixers do not require external energy: the mixing process relies entirely on molecular diffusion. Therefore, in this case, it was the biggest channel size that had the slowest flow velocity and got the best performance of mixture requiring the shortest distance in the mixing area.

In case 4, with higher mass flow rate in both inlet as 0.07 Kg/s, by increasing 10 times of mass flow rate from case 2, the central velocity (Area-Weighted-Average) is also get 10 times bigger (Fig. 7). For l = 0.7 and 1 mm, The two dyeing water are directly pass through the converging, mixing and diverging area without mixing, as shown in Fig. 8. It discloses that with too higher Reynolds number there is no difference between channel sizes, the mixing mechanism becomes dominated by convection rather than diffusion. As Robin H. Liu and Mark A. Stremler [5] revealed, mixing in the straight channel decrease rapidly with increasing Reynolds number due to the corresponding decrease in residence time. For l = 1.3 mm, the two dyeing are mixing well at the end of the mixing area, with comparative bigger

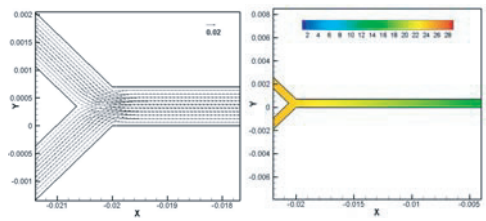

(a) l = 0.7 mm, Re= 0.55

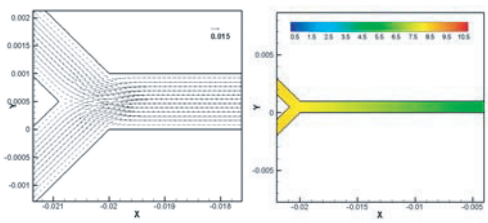

(b) l = 1 mm, Re = 0.53

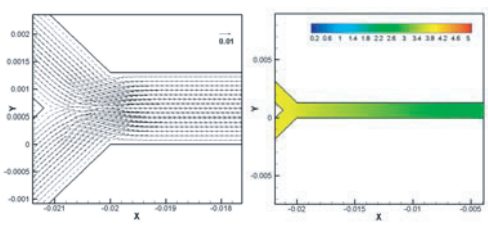

(c) l = 1.3 mm, Re= 0.53

Figure 3: Velocity and Pressure contour

mixing area, lower velocity and pressure drop, these are all advantage for mixing, therefore this case gets the best mixing performance.

By supplying different mass flow rate to Inlet 1 (0.007 Kg/s) and Inlet 2 (0.352 Kg/s) in order to understand the mixing preference in case 5 as shown in Fig. 9. With channel size = 0.7 mm (Fig. 9 (a), (c)), there is a vortex formed in the converging area, the mass flow rate in Inlet 2 is 50 times than Inlet 1, caused the mix overflow in the end of the Inlet 1, the Inlet 1 is almost blocked by Inlet 2. With channel size = 1.3 mm (Fig. 6 (b), (d)), though the Reynolds number are almost the same, the pressure drop in 0.7 mm (302.8 Pascal) is 6 time lower than 1.3mm (50.7 Pascal), hence the Inlet 1 can pass through to the mixing area.

In case 6 (Inlet 1 = 0.070 Kg/s and Inlet 2 = 0.352 Kg/s) as displayed in Fig. 10. With higher mass flow rate input in 0.7 mm, the transition form early from laminar to turbulent flow. Many investigates had focus on the early transition form in micro-channels [8-15].

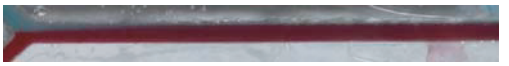

(a) l = 0.7 mm, Re = 0.55

(b) l = 1 mm, Re = 0.55

(c) l = 1.3 mm, Re = 0.53

Figure 4: Mixing performances in each cases

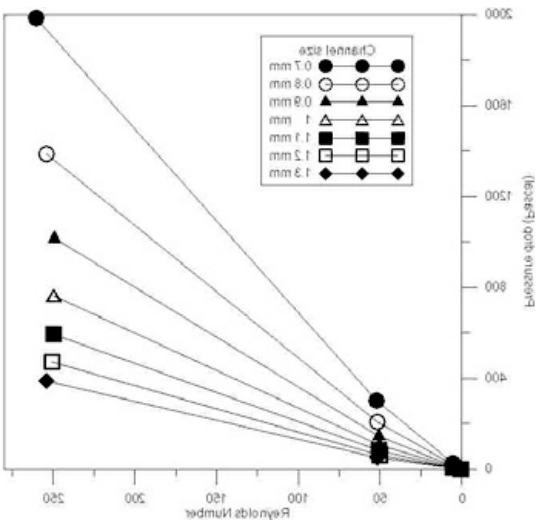

Figure 5: Pressure drop to Reynolds number

Mehendale et al. [8] noted that for the early transition form laminar to turbulent flow in micro-scale tubes, the properties of the liquid change markedly as the fluid flows along the channel so that Reynolds number at the channel exit could be twice that at the inlet. Therefore, the early transition to turbulence might be partially attributed to the variation in Reynolds number. For l = 1 and 1.3 mm, till the end of the mixing zoon, two dyeing water are not mixing well, the blue one flows to the outlet 2 obviously. With supplying different mass flow rate in case 3, 5 and 6, by increasing channel size, the pressure difference between Inlet 1 and Inlet 2 get lower, (as shown in Fig. 11) consequently, in case 6, the smaller channel size acquires better performance of mixture. However, in case 5, the pressure difference between Inlet 1 and Inlet 2 is higher than case 6, but the difference is the mass flow rate, it is too high, Inlet 1 is blocked by Inlet 2 resulting in a bad mixing preference.

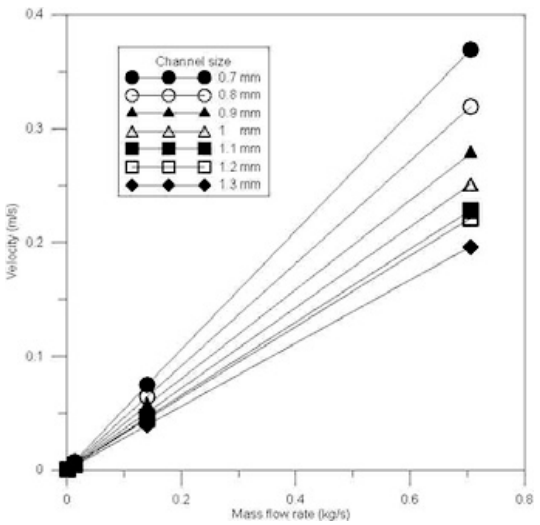

Figure 6: Velocity to mass flow rate

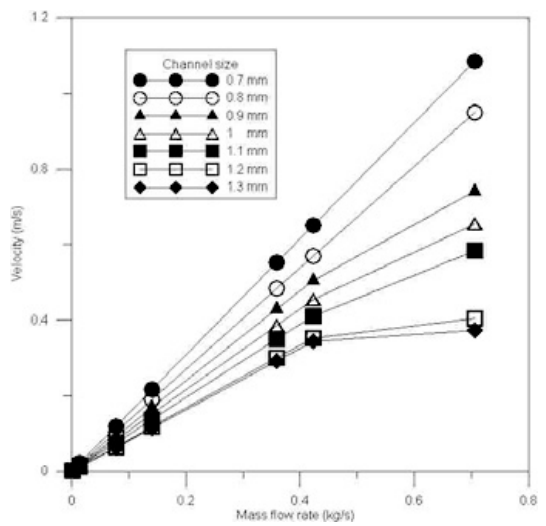

Figure 7: Central velocity to Mass flow rate

In case 7, with mass flow rate in both inlet as 0.352 Kg/s, as shown in Fig. 12 and 13, for the channel size = 0.7 mm, because of the unsteady flow (as shown in Fig. 12), it mixed very well. For l = 1 and 1.3 mm, the performance of mixing gets worse or even not mix, the two dyeing water are directly pass through the mixer.

The results of temperature gradient remain the same trend with the velocity flow pattern. In case 1 and case 2, two fluids of different temperature mixed pretty well (Fig 14). From the temperature contour, it is the biggest channel size that has the best performance of mixture requiring the shortest distance in the mixing area. In case 4 and case 7, as shown in Fig 15, when increasing the mass flow rate, two fluids of different temperature did not mix well. The

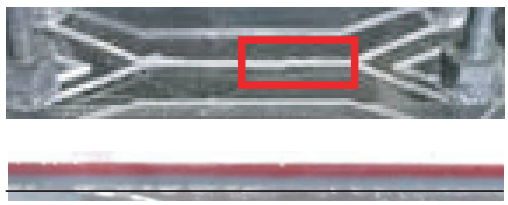

(a) l = 1 mm

(b) l = 1.3 mm

Figure: 8 Mixing performances in each cases

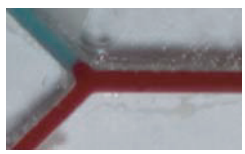

(a) l = 0.7 mm

(b) l = 1.3 mm

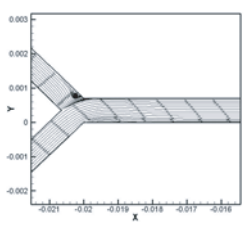

(c) Re=300.01

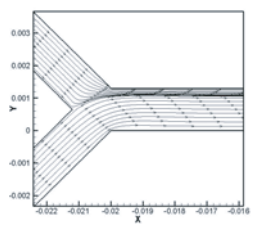

(d) Re= 220.17

Figure 9: Mixing performances in each cases

results of supplying the same mass flow rate in both inlets shows that (Fig 16), the mixing preference decreased when increased the mass flow rate. According to the numerical simulation results, in case 1 and case 2, both outputs are mixed well at 295 K, but when increased the mass flow rate over 0.007 kg/s, the mixing preference got worse, the temperatures of both outputs are similar to both inputs. Compare experimental data with numerical simulation, the temperatures of experiment are all higher than numerical simulation (the average is about 1K). The reason is, though all syringes, pipes, and mixer are covered with 1 inch thermal protector, the temperature is adopted at the time when the mixing processing is at 5 minutes, and then there still has the heat loss (outdoor temperature is around 300 K). Linan Jiang and Man Wong [16] also discovered that, as long as the flow is in either single-liquid or two-phase, the forced convection heat transfer results in a moderate increase of the device temperature with increasing input power. On the other hand,

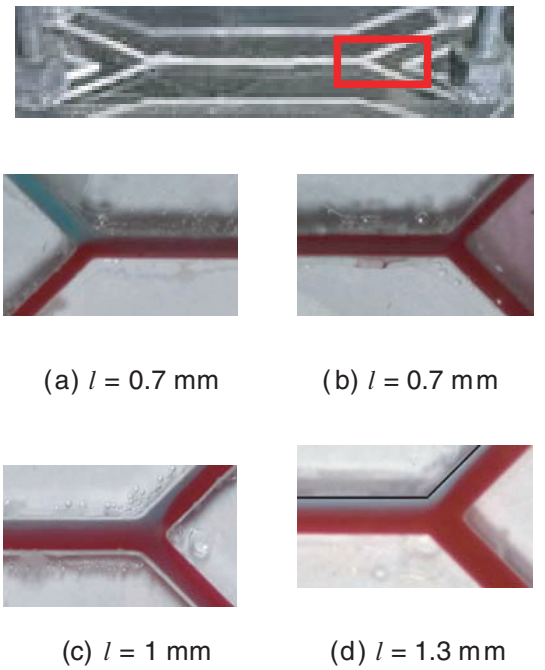

(a) l = 0.7 mm (b) l = 0.7 mm

(c) l = 1 mm (d) l = 1.3 mm

Figure 10: Mixing performances in each cases

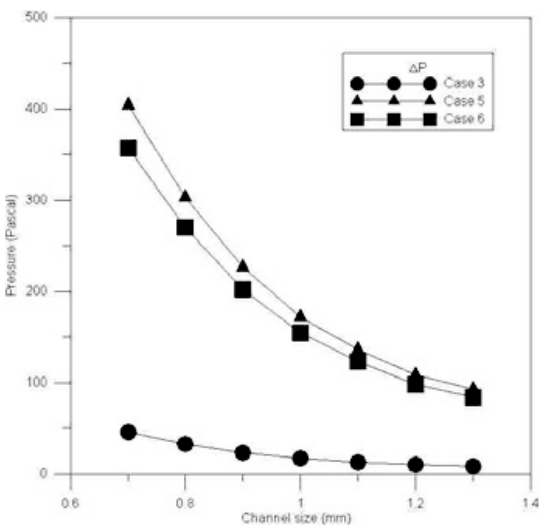

Figure 11: Pressure difference between Inlet 1 and Inlet 2

Fig 17 disclosed the mixing preference of supplying different mass flow rate to Inlet 1 and Inlet 2. In case 3, case 5, and case 6; for Inlet 2 is five times or more over than Inlet 1, the both output temperatures are nearly the same as the bigger flow (Inlet 2). It can be said, there is no difference in changing the channel size in heat transfer, the effect factor of the mixing preference only depends on the mass flow rate.

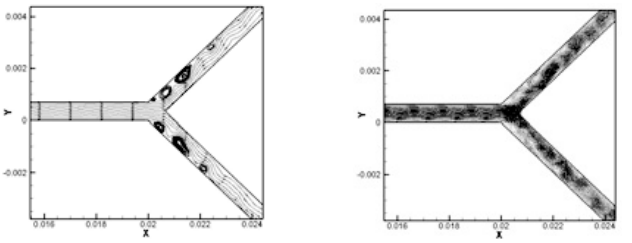

(a) Stream line (b) Velocity contour

Figure 12: Flow pattern in l = 0.7 mm

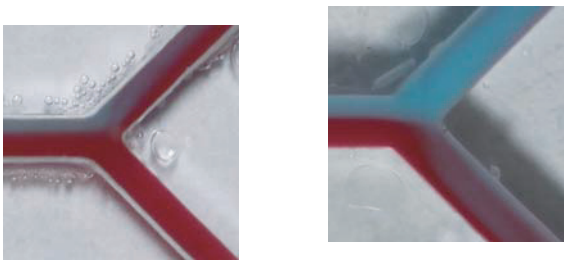

(a) l = 1 mm (b) l = 1.3mm

Figure 13: Mixing performances in case 7

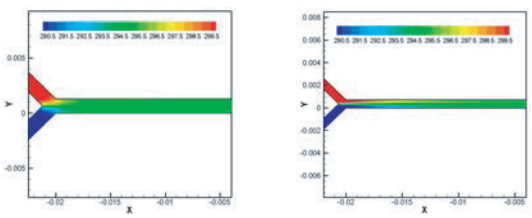

(a) l = 1.3 mm Case1 (b) l = 0.7 mm Case2

Figure 14: Temperature contour in converging area

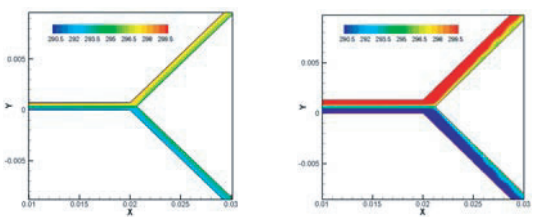

(a) l = 0.7 mm Case4 (b) l = 1.3 mm Case7

Figure 15: Temperature contour in diverging area

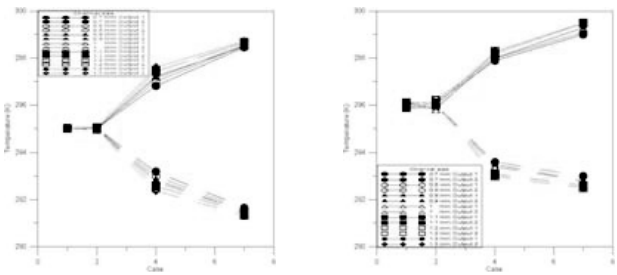

(a) Numerical simulation (b) Experiment

Figure 16: Temperatures of outputs in case1, 2, 4, and 7

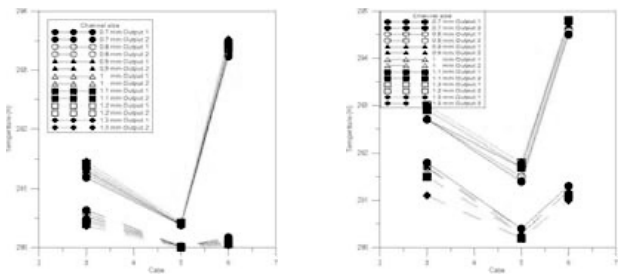

(a) Numerical simulation (b) Experiment

Figure 17: Temperatures of outputs in case 3, 5, and 6

4. CONCLUSIONS

In this paper, we reported on design, numerical simulation, flow visualization, and temperature distribution of X-shaped micro-channels at a wide mixing range of Reynolds number from 1.06 to 514. The simulation results show a congruency with the experiments and the references. At the X-shaped micro-channels with different channel size, the following phenomena occur. (1) At the same mass flow rate as the Reynolds number below 112.53, the biggest channel size had the slowest flow velocity and got the best mixing performance; as the Reynolds number above 112.53, the smaller the channel sizing, the lower the pressure drops and the faster velocity becomes. The transition form early from laminar flow, the unsteady flow is an advantage for mixing in the limited mixing area, therefore 0.7 mm got the best mixing performance. (2) As the mass flow rate is increased, the flow velocity gets higher and takes longer distance in the mixing area at the same channel size. (3) When the mass flow rate is over 0.07 Kg/s, the performance of the mixture gets worse or moreover undivided. (4) As the different mass flow rate input in Inlet 1 and Inlet 2, the smaller channel size gets the better performance of mixture. In case 6, focusing only on Output 1, with l = 1.3 mm, the two fluids of dyed water do not mix well. However, with l = 0.7 mm, the two fluids of dyeing water mix pretty well.

These results clearly indicate that there are many differences between the Reynolds number, and channel size. Further studies should be conducted on the PIV (Particle Image Velocimetry) measurement to compare with the simulation results.

REFERENCES

[1] ZHANG Shanliang, LIN Jianzhong, ZHANG Weifeng, Numerical Research on the Fiber Suspensions in a turbulent T-shaped Branching Channel Flow, *Chin. J. Chem. Eng.,* **15**(1) 30–38 (2007)

[2] Cheng-Chi Chang, Yue-Tzu Yang, Tzu-Hsiang Yen, Chaío-Kuang Chen, Numerical investigation into thermal mixing efficiency in Y-shaped channel using Lattice Boltzmann method and field synergy principle, International Journal of Thermal Sciences **48** (2009) 2092–2099

[3] GUO Wei-Dong, Three-Dimensional Simulation for Effects of Bed Discordance on Flow Dynamics at Y-Shaped Open Channel Confluences, Journal of Hydrodynamics Ser.B, 2007, **19**(5):587–593

[4] Shakhawat Hossain, M.A. Ansari and Kwang-Yong Kim, Evaluation of the mixing performance of three passive micromixers, Chemical Engineering Journal Volume 150, Issues 2–3, 1 August 2009, Pages 492–501

[5] Robin H. Liu, Mark A. Stremler, Kendra V. Sharp, Michael G. Olsen, Juan G. Santiago, Ronald J. Adrian, Hassan Aref, and David J. Beebe, Passive Mixing in a Three-Dimensional Serpentine Microchannel, Journal of Microelectronachanical Systems, VOL. 9, NO. 2, JUNE 2000

[6] S. Mahabunphachai, M. Koç, Fabrication of Micro-Channel Arrays on Thin Metallic Sheet Using Internal Fluid Pressure: Investigations on Size Effects and Development of Design Guidelines," Journal of Power Sources, vol. 175, no. 1, pp. 363–71, 2008.

[7] B. -X. Wang and X. F. Peng. "Experimental Investigation on Liquid Forced-Convection Heat Transfer Through Microchannels," Int. J. Heat Mass Transfer, Vol. 37, Suppl.1, pp. 73–82, 1994.

[8] Mehendale, S.S., Jacobi, A.M., Shah, R.K., Heat Exchangers at Micro- and Meso-scales. In: Proceedings of the International Conference on Compact Heat Exchangers and Enhance Technology for the Process Industries, Banff, Canada, 1999. pp. 55–74

[9] Webb, R.L. and Zhang, M., Heat Transfer and Friction in Small Diameter Channels. Microscale Thermophys. Eng. **2**, pp. 189–202.

[10] Johan, K. et al., 2001, Liquid Transport Properties in Sub-micron Channel Flows. In: Proceedings of 2001 ASME International Mechanical Congress and Exposition, New York, NY, November 11–16, 2001

[11] Wu, P.Y. and Little, W.A., Measurement of the Heat Transfer Characteristics of Gas Flow in Fine Channel Heat Exchangers Used for Microminiature Refrigerators. Cryogenics **24**, pp. 415–420, 1984.

[12] Mala, G.M. and Li, D, Flow Characteristics of Water in Microtubes. Int. J. Heat Fluid Flow **20**, pp. 142–148, 1999.

[13] Gad-ed-Hak, M., The Fluid Mechanics of Microdevices—the Freeman scholar lecture. J. Fluid Eng. **121**, pp. 5–33, 1999.

[14] Drain, K. et al., 1995. Single Phase Forced Convection Heat Transfer in Microgeometries—a review. In: Proceedings of 30th Intersociety Energy Conversion Engineering Conference, Florida, 1995.

[15] Kemler, E., A Study of The Data on The Flow of Fluids in Pipes. Trans. ASME 55, pp. 7–32 paper Hyd-55–2, 1933.

[16] Shah, R.K. and London, A.L., Laminar Flow Forced Convection in Ducts. In: Irvine, T.F. and Hartnett, J.P., Editors, 1978. Advances in Heat Transfer (Suppl. 1), Academic Press, New York, San Francisco, London.

[17] Linan Jiang, Man Wong, Yitshak Zohar, Phase Change in Microchannel Heat Sinks with Integrated Temperature Sensors, Journal of Microelectromechanical System, **8** 358, 1999.

[18] C. B. Sobhan and S. V. Garimella, A Comparative Analysis of Studies on Heat transfer and Fluid Flow in Microchannels,' Proceedings of the Micro-Scale Heat Transfer Conference, Alberta, Canada, pp.80–92, 2000.

[19] S. K. Clark and K. D. Wise, Pressure Sensitivity in Anisotropically Etched Thindiaphragm Pressure Sensors, IEEE Trans. Electron Devices, Vol. ED-26, pp.1887–1896 1979.

[20] S. Sugiyama, K. Shimaoka, and O. Tabata, Surface Micromachined Micro-Diaphragm Pressure Sensors, in Proc. 6th Int. Conf. Solid-State Sensors and Actuators (Transducer'91), pp.188–191, 1991.

[21] Celata, G.P., Cumo, M., Gulielmi, M. and Zummo, G., 2000. Experimental Investigation of Hydraulic and Single Phase Heat Transfer in 0.130 mm Capillary Tube. In: Celata, G.P. et al., 2000. Proceedings of the International Conference on Heat Transfer and Transport Phenomena in Microscale, Begell House, Inc., New York, pp. 108–113.